Gradient-Free Stochastic Sensitivity Analysis of the Shipboard Power System

P. Prempraneerach[1], J. Foo[2], M.S. Triantafyllou[1], C. Chryssostomidis[1]
and G.E. Karniadakis[1,2]
[1] **Department of Mechanical Engineering**
Massachusetts Institute of Technology, Cambridge, MA 02139
[2]**Division of Applied Mathematics**
Brown University, Providence, RI 02912

Abstract

Sensitivity analysis results are useful both for the early design stage – where the parametric space can be substantially reduced – but also in operating conditions, e.g. of the future electric ship, resulting in reduced operational costs and increased reliability. Here we discuss variance-based methods to analyze the sensitivity of stochastic electro-mechanical systems with multirate dynamics. We present results for an illustrative example and for a model of an integrated power system.

1. INTRODUCTION

In the All-Electric Ship (AES), there is an increasing demand for electric power for ship system automation, electrical weaponry, electric propulsion, and ship service distribution. About 70% to 90% of power from the generator units in the fully integrated power system (IPS) is consumed in the propulsion systems [2]. Many machines and electrical components form the power generation and propulsion drives in the AES. As a result, *sensitivity analysis* that can identify the influential and interactive parameters from a large number of parameters is needed for the IPS designer to improve performances of the integrated system and to prevent a cascaded failure. Sensitivity analysis, based on the "One-At-a-Time" (OAT) stochastic variation [9], has been shown to be able to identify and prioritize the important parameters of an AC subsection in the entire IPS [6]. In addition, to further accelerate large-scale simulation or even guide experimental studies, a reduction of parametric space can be accomplished by fixing the less important parameters at their nominal values.

The two main classes of techniques for ranking these inputs in sensitivity studies are *local* and *global* methods. The local approach [5, 10], which relies on a partial derivative of output with respect to input, is used to measure the sensitivity around a local operating point. When the system has strong nonlinearity and the input uncertainties are contained within a wide range, the local sensitivity does not provide full information to the IPS designer. On the other hand, the global approach examines the sensitivity from the entire range of the parameter variations. The screening methods, which are included in the global methods, rank the important factors and their interaction among a large number of system parameters. These screening techniques are based on OAT perturbation of parameters, which directly yields the main input effect without input interaction. Several screening methods have been proposed in the literature, for example, the Morris method [7, 12], Cotter's method [3], factorial experimentation [1], and iterated fractional factorial design [11]. The different aproaches have their strengths and weaknesses. The Morris method can efficiently identify the sensitive parameters when a system has a large number of inputs or parameters. Only the worst-case analysis of a system is examined for the upper and lower bounds of system variables in Cotter's method. In factorial experimentation, all combinations of inputs' interactions as well as the main effects are evaluated at the same time, which requires intensive computation. Iterated fractional factor design reduces this large input-combination computation by evaluating only important combinations. As a result, the sensitivity indices might be biased.

In [8], four sensitivity analysis techniques for ranking the inputs' significance and the nonlinear and coupling effects of inputs were studied. Two of them were based on gradient-based analysis while the other two were based on variance-based analysis. Gradient-based methods, while effective in general, can be very costly and not so accurate for non-smooth solutions. The regularity required for computing the local gradient at one point in a parameter range to be representative of the gradient over the entire range is not guaranteed nor expected for a nonlinear system like IPS. To this end, in this paper we focus on variance-based methods and examine their connection to gradient-based methods, their accuarcy, and their effectiveness in a small-scale IPS typical of the AES.

2. SENSITIVITY ANALYSIS METHODS

A new approach to simulate the IPS subject to uncertainty was introduced in [8] based on the concept of generalized Polynomial Chaos (gPC) method [13]. The most efficient approach for such nonlinear systems is the collocation projection, and we will refer to the corresponding method as *probabilistic collocation method* (PCM). This approach is as sim-

ple as the standard Monte Carlo approach but the sampling points are specific points related to the roots of the orthogonal polynomials invcolved in the expansion basis of gPC. A more efficient extension developed in [4, 8] is based on multi-elements (MEPCM version), where the parametric space is further subdivided into non-overlapping subdomains ("elements") whithin which gPC expansions are employed. Another useful option is the use of full-grids or sparse-grids in PCM or in MEPCM, see [8].

2.1. Connection to gradient-based methods

In this section we make some mathematical connections between MEPCM local variance-based sensitivity techniques and gradient-based methods. Let us focus on a particular hypercube element B, a subset of the N-dimensional parametric space, written without loss of generality as the product set $\prod_{i=1}^{N}[x_{0,i}-h,x_{0,i}+h]$ where $x_0 = (x_{0,1},x_{0,2},...,x_{0,N})$ is the center of B. Suppose we have a function $f \in C^3(B)$ and assume X is a random variable uniformly distributed on B. We will show that the variance of $f(X)$ over B^i, when normalized with the one-dimensional uniform distribution variance, approximates the norm of the gradient $||\nabla f|_{x_0}||^2$ in the limit as $h \to 0^+$. This result is easily generalizable to rectangular B, but we will assume uniform edge lengths for simplicity here.

We begin with the multi-dimensional Taylor expansion:

$$
\begin{aligned}
f(x) &= f(x_0) + \sum_{|\alpha|=1} \left.\frac{\partial^\alpha f}{\partial x^\alpha}\right|_{x_0}(x-x_0)^\alpha \\
&\quad + \frac{1}{2!}\sum_{|\alpha|=2}\left.\frac{\partial^\alpha f}{\partial x^\alpha}\right|_{x_0}(x-x_0)^\alpha \\
&\quad + \frac{1}{3!}\sum_{|\alpha|=3}\left.\frac{\partial^\alpha f}{\partial x^\alpha}\right|_{x_0}(x-x_0)^\alpha + O(x-x_0)^4,
\end{aligned}
$$

where α is a multiindex of dimension N. In other words, $\alpha = (\alpha_1,\alpha_2,...,\alpha_N)$, $\alpha_i \in \mathbb{N}$, and $|\alpha| = \alpha_1 + \cdots + \alpha_N$. Let $\int_{x_0-h}^{x_0+h}f(x)dx$ denote the N-dimensional integral of f over B. Then, we can obtain the second moment as (see [4] for details),

$$
\begin{aligned}
\frac{1}{(2h)^N}\int_{x_0-h}^{x_0+h}f(x)^2dx &= f(x_0)^2 + \sum_{i=1}^{N}\frac{h^2}{6} \\
&\quad \left(2\left.\frac{\partial f}{\partial x_i}\right|_{x_0}^2 + 2f(x_0)\left.\frac{\partial^2 f}{\partial x_i^2}\right|_{x_0}\right) \\
&\quad + o(h^4) \\
&:= \mathbb{E}_B[f(X)^2].
\end{aligned}
$$

Similarly, we obtain the first moment and thus the variance of f over the element B:

$$
\mathrm{Var}_B[f(X)] = \frac{h^2}{3}||\nabla f|_{x_0}||^2 + o(h^4).
$$

Note that $\frac{h^2}{3}$ is the variance of the one-dimensional distribution of the underlying variable X, and

$$
\frac{\mathrm{Var}_B[f(X)]}{\frac{h^2}{3}} = ||\nabla f|_{x_0}||^2 + o(h^2).
$$

The rate of convergence here is $o(h^2)$, which is independent of N. Hence, we see that the variance-based sensitivity analysis is related to the gradient-based sensitivity analysis as indicated in the above relationship.

2.2. Variance Method

The Variance method introduced here directly takes advantage of the efficiency and accuracy of the PCM to identify each input sensitivity and input interaction. This method relies on a variation of the output when only one input is a random variable instead of using the approximated gradient to measure the sensitivity of each input. Note that here we use the standard deviation as a sensitivity index when we refer to the Variance method. First, let us define the *variance effect* (VEE_i) of each input on the output, $y^j(x_1,...,x_k)$ for $j = 1,...,n$, as:

$$
\begin{aligned}
VEE_i^j &= E_{x_{i\neq j}}[\sigma_{x_i}[y^j(\mathbf{x})]] \qquad\qquad (1)\\
&= \int_{x_1}\cdots\int_{x_{i-1}}\int_{x_{i+1}}\cdots\int_{x_k} \\
&\quad \sigma_{x_i}[y^j(\mathbf{x})]dx_1\cdots dx_{i-1}dx_{i+1}\cdots dx_k,
\end{aligned}
$$

where σ_{x_i} denotes the standard deviation of the j output ($y^j(\mathbf{x})$) when only x_i input is a random variable and the other inputs are fixed at the collocation points in the $k-1$ input dimension. $E_{x_{i\neq j}}[\,]$ represents an expectation of all other inputs except the x_i input. Formulating an OAT variation of each input in this way, the *interaction* of the x_i input with the others, called IEE_i, can be described by

$$
IEE_i^j = \sigma_{x_{i\neq j}}[\sigma_{x_i}[y^j(\mathbf{x})]] =
$$

$$
\sqrt{\int_{x_1}\cdots\int_{x_{i-1}}\int_{x_{i+1}}\cdots\int_{x_k}(\sigma_{x_i}[y^j(\mathbf{x})]-VEE_i)^2dx_1\cdots dx_{i-1}dx_{i+1}\cdots dx_k}.
$$

Here $\sigma_{x_{i\neq j}}[\,]$ denotes a standard deviation of all other inputs except the x_i input. The magnitude of IEE_i can only specify the coupling of the i parameters without taking into account the nonlinearity of the x_i term. Figure 1 demonstrates how to obtain the elementary and coupling effects from the standard deviation of each x_i input in the case of three input parameters. The computational cost to obtain VEE_i is approximately $O(N_c^k \times k)$, where N_c is the number of collocation points per direction.

This technique can be further applied to compute the sensitivity of input parameters in a system of ODEs by solving N_c
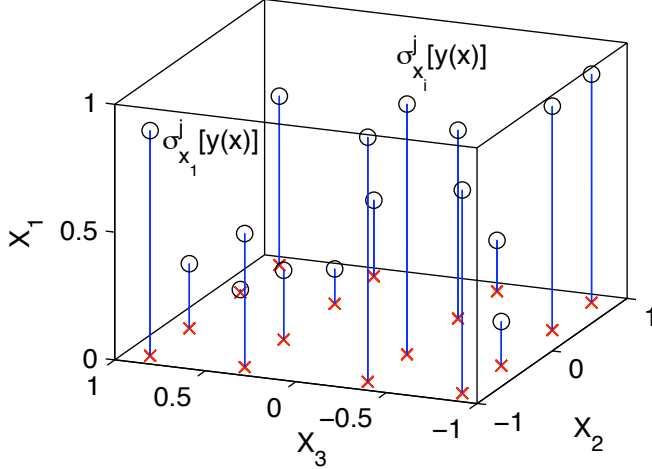
Figure 1. With $N_c = 4$ collocation points in the full-grid PCM, the standard deviation of the x_1 input is computed at the full-grid collocation points, where x_2 and x_3 are assumed to be independent random variables, such that the elementary effect and interaction of x_1 with the other inputs can be uncovered.

ODEs for one input at each time step; thus, with k inputs, we need to solve a total of N_c^k ODEs for the OAT sensitivity as well as parameter interaction. Similar to the stationary case, we compute the standard deviation of the system integration with respect to the x_i using one-dimensional full-grid PCM, while all other inputs are fixed at the collocation points of the $k-1$-dimensional full-grid PCM. Then, we compute the standard deviation of σ_{x_i} with respect to $x_{i \neq j}$ for measuring the parameter interaction.

2.3.   Inverse Variance Method

Consider the dual concept of the Variance method just described. This technique examines the inverse of how unimportant each input parameter is in the system output, $y^j(x_1,\ldots,x_k)$, which is related to the first-order effect. Let us define the first-order effect of the x_i input as $IVEE_i$, as:

$$IVEE_i^j = \frac{1}{E_{x_i}\left[\sigma_{x_{i \neq j}}[y^j(\mathbf{x})]\right]}, \qquad (2)$$

where the denominator is defined as

$$E_{x_i}\left(\sqrt{\int_{x_1}\cdots\int_{x_{i-1}}\int_{x_{i+1}}\cdots\int_{x_n}\left(y(\mathbf{x}|x_1,\ldots,x_{i-1},x_{i+1},\ldots,x_k)\right.}\right.$$

$$\left.\left.\overline{-E_{x_{i \neq j}}[y(\mathbf{x})]}\right)^2 dx_1\cdots dx_{i-1}dx_{i+1}\cdots dx_k\right),$$

where $\sigma_{x_{i \neq j}}[y^j(\mathbf{x})]$ is the standard deviation of the output when all inputs except the i input are random variables, which

is described as the negligible effect of the x_i input on the output. $E_{x_i}[\,]$ represents the expectation of the i input. An inverse of the $E_{x_i}[\sigma_{x_{i \neq j}}[f(\mathbf{x})]]$ specifies the importance effect of the x_i input. Likewise, the coupling effect of the i input with the other inputs can be examined from the $IIEE_i$, defined below:

$$IIEE_i^j = \sigma_{x_i}[\sigma_{x_{i \neq j}}[y^j(\mathbf{x})]], \qquad (3)$$

where $\sigma_{x_i}[\,]$ stands for the standard deviation of the i input. Similar to the Variance method, $IIEE_i$ can only capture the coupling effect of i input with the others, not the nonlinearity associated with x_i. According to these definitions, the sparse-grid PCM can be directly employed for computing $\sigma_{x_{i \neq j}}[\,]$, especially for large input dimensions. Owing to the efficiency of the full-grid PCM in a small input dimension, $E_{x_i}[\,]$ and $\sigma_{x_i}[\,]$ can be computed with the Gauss quadrature. Therefore, this technique can provide fast convergence of $IVEE_i$ and $IIEE_i$ accuracy with less computational cost, particularly in cases with high input dimension. The total computational cost is in the order of $O(n(L,k-1) \times Nc \times k)$, where $n(L,k-1)$ is a number of collocation point at level, L, in $k-1$ input dimension. Thus, the computational cost of this method should be several orders of magnitude smaller than that of the Variance method when k is large; in the Variance method only a full-grid PCM can be used.
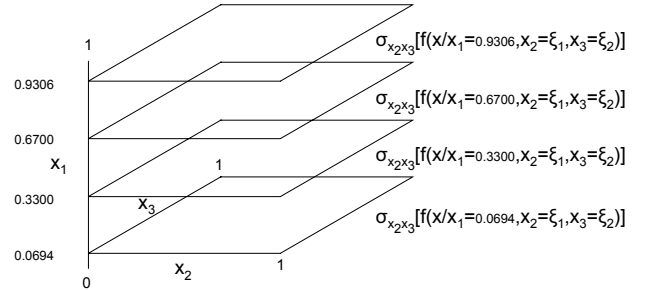

Figure 2. For the full-grid PCM with $Nc = 4$ in the first direction, the standard deviation of x_2 and x_3 inputs is computed at the sparse-grid collocation points, where the x_1 is assumed to be fixed at the full-grid collocation point. The inverse of the mean of σ_{x_2,x_3} with respect to x_1 can identify the elementary effect of x_1, while the standard deviation of σ_{x_2,x_3} with respect to x_1 specifies the coupling effect of x_1 with the others.

To explain the concept of this method in a three-dimensional input space, Figure 2 shows how to obtain the effect of excluding the x_1 input by considering the standard deviation of x_2 and x_3 with fixed x_1 at the full-grid collocation points. The inverse of the mean of $\sigma_{x_2,x_3}[f(\mathbf{x}/x_1$ is fixed, $x_2 = \xi_1, x_3 = \xi_2)]$ with respect to x_1 can be used to rank the significance of the x_1 input. Moreover, the standard devi-

ation of this quantity with respect to x_1 identifies the coupling effect of x_1 with the other inputs.

3. RESULTS
3.1. An illustrative example

Let us first consider a simple polynomial function with x_i being random uniform variables:

$$y_6 = 63x_1^5 x_2 - 70x_2^3 x_3^2 + 15x_1 x_2 x_3 \text{ for } 0 < x_i < 1, \quad (4)$$

In Figure 3 we plot the mean and standard deviation of the elementary effect based on the Variance (upper plot) and Inverse Variance (lower plot) methods. We see that the ranking of the inputs is the same according to the VEE_i and $IVEE_i$, respectively, and in fact they agree with results obtained with the gradient-based methods, see [8]. The first input (x_1) is the most sensitive due to the fifth order polynomial, while the sensitivities of x_2 and x_3 are ranked second and third. However, the interaction effects obtained with the two methods are different with the Variance method closer to the gradient-based methods but with the Inverse Variance method producing erroneous results with respect to interaction. For other cases for example, e.g. the Morris function [8], where only interaction terms are involved but not powers of the same variable, both methods (i.e., including the Inverse Variance method) give correct results for the interaction effect as well. In terms of computation time, the Inverse Variance method is at least an order of magnitude faster.

From this and several other example with high-dimensional functions and parametric ODEs presented in [8] we have drawn the following conclusions:

• *Variance Method*: The relative magnitude of VEE_i can rank the sensitivity of inputs. The magnitude of IEE_i captures only the coupling of inputs. It does not include the inputs' nonlinearity because of the OAT variance measurement of a single random variable. Using the efficiency of the full-grid PCM, the convergence rate of the sensitivity index is exponential in a small dimension problem; however, this rate is sensitive to the function's monotonicity.

• *Inverse Variance Method*: The relative magnitude of $IVEE_i$ can correctly rank the sensitivity of inputs as well. Similar to the Variance method, the magnitude of $IIEE_i$ can capture only the coupling of inputs, but not the inputs' non-linearity. Furthermore, the value of $IIEE_i$ is also sensitive to the function's monotonicity due to the possibility of cancellation effect in computing the standard deviation of the $n-1$ inputs in the n-dimensional problem. The main advantage of this technique is its rapid convergence rate of the sensitivity index and its independence in convergence characteristic from any kind of the inputs' nonlinearity. The drawback is that it does not give the correct interaction effect and hence it leads to erroneous trajectories in solving parametric ODEs.
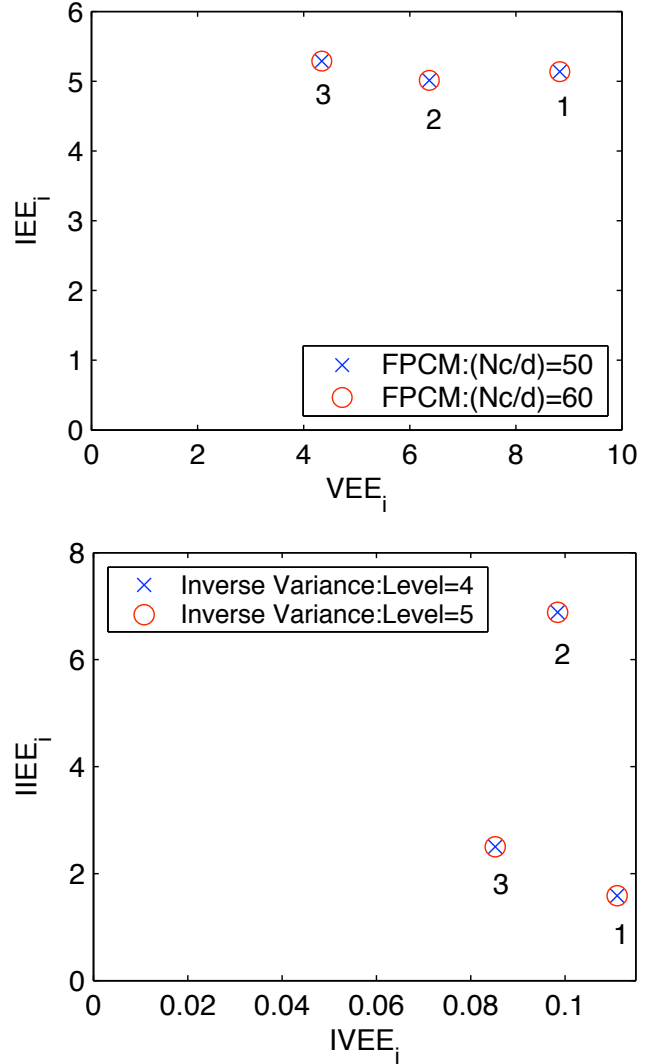

Figure 3. Function (y_6): the mean and standard deviation of EE_i from the Variance method with $Nc/d = 10$ and 20 (upper), and from the Inverse Variance method with $Nc = 8$ and $Level = 4$ to 5 (lower). The two methods give the same ranking but different interaction of parameters.

Table 1. Parameters of a 200-hp induction machine

Parammeters in [p.u]					
r_s	X_{ls}	X_m	X'_{lr}	r'_r	H
0.01	0.0655	3.225	0.0655	0.0261	0.922

3.2. An open-loop induction machine with an infinite bus

Here we analyze the sensitivity of a model IPS with ten input parameters in the configuration shown in Figure 4. The machine equations are expressed in a qd0-synchronous reference frame. The equations of this three-phase system with quadratic nonlinearities consist of seven state variables: three rotor reactances $[\psi'^e_{qr}, \psi'^e_{dr}, \psi'^e_{0r}]$, the rotor's angular velocity $[\omega_r]$, and three stator or tie-line currents $[i^e_{qt}, i^e_{dt}, i^e_{0t}]$ (see Equation 4-23 to 4-29 in [8]). Two states, ψ'^e_{0r} and i^e_{0t}, are uncoupled from the others. All parameters, given in Table 1, are lumped into α_i variables for a simplification of state equations. The detailed derivation of system modeling can be found in [8]. The start-up dynamics of a 200-hp induction machine in an open-loop configuration, considered here for $t \in [0,3]$ seconds, includes fast transient dynamics from electrical components, stator and rotor windings, and slow dynamics of a mechanical subsystem, a rotor inertia.
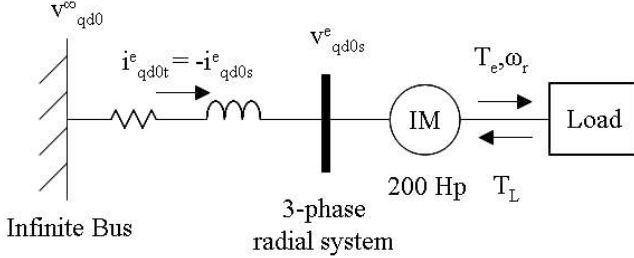

Figure 4. A one-line diagram of the induction machine connected to the infinite bus through a RL tie line.

Because of the five coupled output variables, $[\psi'^e_{qr}, \psi'^e_{dr}, \omega_r, i'^e_{qt}, i'^e_{dt}]$, the trajectories of 10 input parameters, including $[r_s, x_{ls}, x_m, x'_{lr}, r'_r, r_t, L_t, M_t, T_{load}, H]$, are shown only for the d-axis tie line current or i^e_{dt} state shown in Figure 5. All these inputs are assumed to be independent random variables with 10 percent variation from their mean or nominal values. Using the Variance method, the normalized sensitivity trajectories of these 10 inputs indicate which inputs have larger impact on the output, such as i'^e_{dt}, as shown in Figure 5. In particular, i^e_{dt} is very sensitive to multiple inputs, especially x_{ls} and x'_{lr} in the first second and r'_r right before reaching the synchronous speed. These sensitivity indices reflect the *multi rate* dynamics associated

with the induction machine. Initially during the first second, the stator and rotor windings attempt to accelerate the rotor up to speed; therefore, the reactance of these windings, x_{ls} and x'_{lr}, should be the most sensitive parameters during the electrical transient regime. After the electrical transient dies out, the rotor inertia, H, and mechanical torque load, T_{load}, also have significant influence on the tie line or stator current during [1,2] seconds, where the mechanical time scale dominates. In terms of input coupling, all these five parameters $(r'_r, x_{ls}, x'_{lr}, H, T_{load})$ exhibit strong interaction with other inputs. At each time step, the IEE_i versus VEE_i plot can be used to directly rank the inputs' sensitivity as well as interaction, as shown in Figure 6 during the electrical transient (upper) and during the mechanical transient (lower). Notice that r_t, L_t, and M_t from the tie line and x_m from the induction machine have almost a negligible effect on this i'^e_{dt} output because the infinite bus absorbs all variations in the tie line's parameters. The mutual flux leakage, x_m, is usually about 100 times larger than the flux leakage of the stator and rotor windings; thus, with the same percentage of fluctuation, x_m is less sensitive than x_{ls} and x'_{lr}.
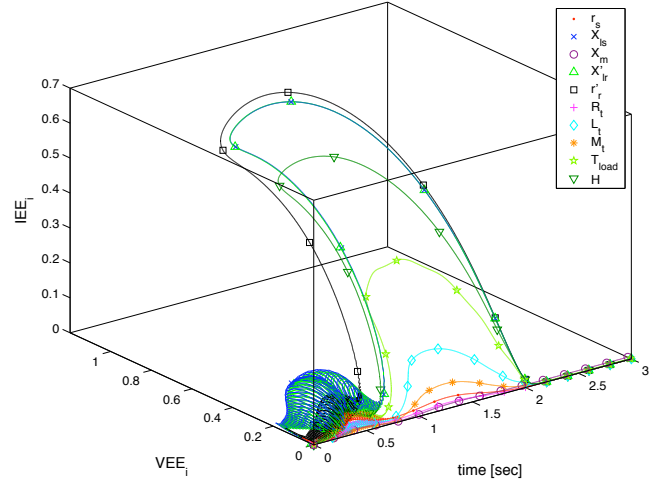

Figure 5. For the y_5 variable or i'^e_{dt}, VEE_i and IEE_i trajectories of all 10 input parameters as a function of time, $t \in [0,3]$ second, using the Variance method with $(Nc/d) = 20$.

To summarize the i input sensitivity on all j system outputs over the entire time interval in a two-dimensional figure, we need to define an average sensitivity index as the $(ES_{2,(j,i)})$ and an average interaction index as the $(SS_{2,(j,i)})$, using the L_2 norm:

$$ES_{2,(j,i)} = ||E[EE_i]||_2 \text{ and } SS_{2,(j,i)} = ||\sqrt{E[EE_i]^2 + \sigma[EE_i]^2}||_2.$$
$$(5)$$

However, because some parameters might have strong influences only within a specified time interval, the peak sensitivity $((ES_{\infty,(j,i)}))$ and interaction indices $((SS_{\infty,(j,i)}))$, de-
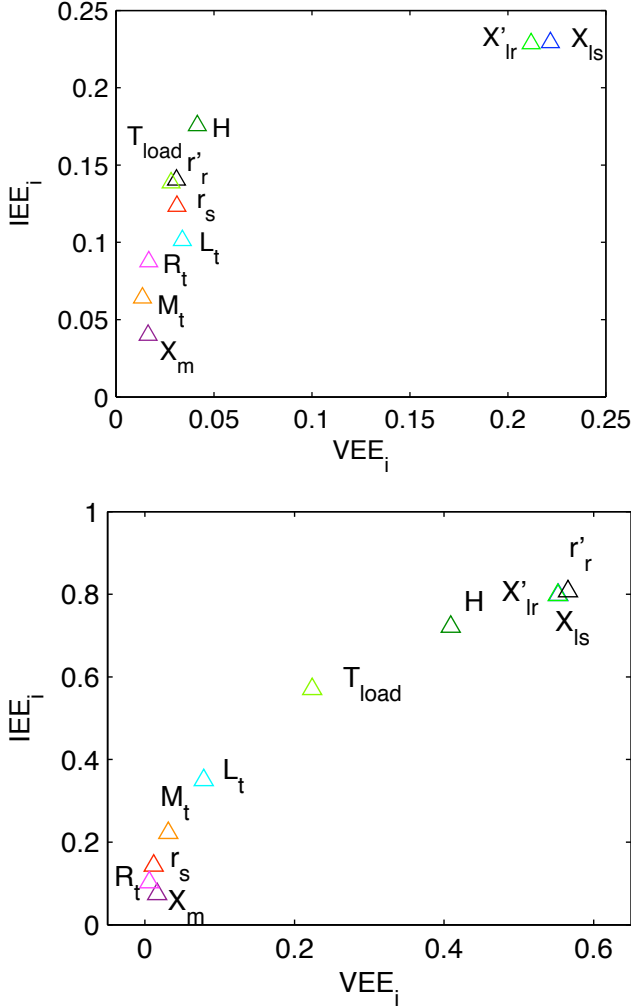
fined below, must be considered along with the $(ES_{2,(j,i)})$ and $(SS_{2,(j,i)})$.

$$ES_{\infty,(j,i)} = ||E[EE_i]||_\infty \text{ and } SS_{\infty,(j,i)} = ||\sqrt{E[EE_i]^2 + \sigma[EE_i]^2}||_\infty.$$
(6)

Therefore, all the normalized sensitivity trajectories of the induction machines with 5 coupled outputs and 10 input parameters can be obtained by plots of $ES_{2,(j,i)}$ for ranking the input sensitivity, and of $SS_{2,(j,i)}$ for ranking the input interaction; e.g., see plot of $ES_{2,(j,i)}$ between 0 and 3 seconds in Figure 7. Notice that the y_2 or $\psi_{dr}^{'e}$ output is the most sensitive, particularly to the electrical parameters, among all the outputs.
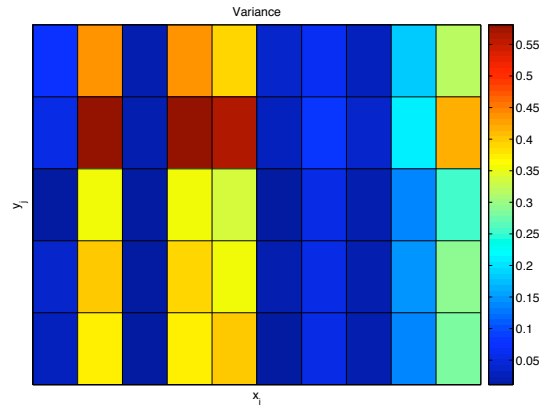

Figure 7. $ES_{2,(j,i)}$ plot using the Variance method for ranking the input sensitivity. The order of x_i inputs on the x-axis are $[r_s, x_{ls}, x_m, x_{lr}', r_r', r_t, L_t, M_t, T_{load}, H]$ from left to right, and the order of y_j outputs on the y-axis are $[\psi_{qr}^{'e}, \psi_{dr}^{'e}, \omega_r, i_{qt}^{'e}, i_{dt}^{'e}]$ from top to bottom.

4. SUMMARY

Sensitivity analysis of integrated power systems (IPS) can be very helpful in ranking the most influential inputs and their interactions. This information can be used in constructing reduced-order models, guide experimental work, and select the proper parameter range in the preliminary stages of designing an IPS. The variance-based methods we presented here do not require any gradient evaluation, and hence they provide an accurate and efficient way of quantifying the sensitivity indices of IPS. Having specified the most important parameters, it may then be desirable to also quantify the *range* within a specific parameter that is the most critical in the response of the IPS. To this end, the multi-element propabilistic collocation method (MEPCM) developed in [4, 8] can be employed in conjunction with an adaptive algorithm that will generate small subdomains (i.e., elements) in regions of the parameter space where the local variance (e.g., integrated

Figure 6. Mean and standard deviation of EE_i from the Variance method, when time is fixed at 0.3 (uuper plot) and 1.5 seconds (lower plot), where the electrical and mechanical transients dominate, respectively.

over an element) is maximum. This algorithm is straightforward to implement, and our results today show that it is also very effective.

ACKNOWLEDGMENT

REFERENCES

[1] Box, G.E.P., Hunter W.G., and Hunter J.S., *Statistics for Experimenters. An Introduction to Design, Data Analysis and Model Building*, Wiley, New York, 1978.

[2] Clayton, D.H., Sudhoff S.D., Grater G.F. ,Electric Ship Drive and Power System, *Conf. Rec. 2000 24th Int. Power Modulation Symp.*, 2000, pp. 85-88.

[3] Cotter, S.C., A screening design for factorial experiments with interactions, *Biometrika*, Vol. 66, pp. 317-320, 1979.

[4] Foo, J., Multi-element probabilistic collocation in high dimensions: Applications to systems biology and physical systems, PhD thesis, Brown University, 2008.

[5] Hockenberry, J.R., Evaluation of Uncertainty in Dynamic, Reduced-Order Power System Models, Ph.D. thesis, Massachusetts Institute of Technology, 2000.

[6] PC Krause and Associates, Power System Control Development, Final Report, Contract F33615-99-D-2974 for NSF/ONR Partnership in Electric Power Network Efficiency and Security (EPNES), March 2003.

[7] Morris, M.D., Factorial Sampling Plans for Preliminary Computational Experiments, *Technometrics*, Vol. 33, No. 2, pp. 161-174, May 1991.

[8] Prempraneerach, P., Uncertainty Analysis in a Shipboard Integrated Power System using Multi-Element Polynomial Chaos, Ph.D. thesis, Massachusetts Institute of Technology, 2007.

[9] Prempraneerach, P., Hover F.S., Triantafyllou M.S., Karniadakis G.E., Uncertainty Quantification in Simulations of Power Systems: Multi-Element Polynomial Chaos methods, *submitted to International Journal of Electrical Power and Energy Systems*, 2007.

[10] Rabitz, H., Kramer M., and Dacol D., Sensitivitiy analysis in chemical kinetics, *Annu. Rev. Phys. Chem.*, Vol. 34, pp. 419-461, 1983.

[11] Saltelli A., Andres T.H., Homma T., Sensitivity analysis of model output. Performance of the iterated fractional factorial design method, *Computational statistics and data analysis*, Vol. 20, No. 4, pp.387-407, 1995

[12] Saltelli A., Chan K., Scott M., *Sensitivity Analysis*, John Wiley & Sons Ltd, 2000.

[13] Xiu, D., Karniadakis G.E., The Wiener-Askey polynomial chaos for stochastic differential equations, *SIAM Journal for Scientific Computation*, Vol. 24, No. 2, pp. 619-644, 2002.